Nanoscale Research Letters

NANO EXPRESS

Open Access

Restored microRNA-326-5p Inhibits Neuronal Apoptosis and Attenuates Mitochondrial Damage via Suppressing STAT3 in Cerebral Ischemia/Reperfusion Injury

Yumin Huang[1], Yingge Wang[2,3,4], Zuowei Duan[2], Jingyan Liang[3,4,5], Yijun Xu[6], Shuai Zhang[2] and Tieyu Tang[2*]

Abstract

Studies have greatly explored the role of microRNAs (miRNAs) in cerebral ischemia/reperfusion injury (CI/RI). But the specific mechanism of miR-326-5p in CI/RI is still elusive. Hence, this study was to unmask the mechanism of miR-326-5p/signal transducer and activator of transcription-3 (STAT3) axis in CI/RI. Two models (oxygen and glucose deprivation [OGD] in primary rat cortical neurons and middle cerebral artery occlusion [MCAO] in Sprague–Dawley rats) were established to mimic CI/RI in vitro and in vivo, respectively. Loss- and gain-of function assays were performed with OGD-treated neurons and with MCAO rats. Afterward, viability, apoptosis, oxidative stress and mitochondrial membrane potential in OGD-treated neurons were tested, as well as pathological changes, apoptosis and mitochondrial membrane potential in brain tissues of MCAO rats. Mitofusin-2 (Mfn2), miR-326-5p and STAT3 expression in OGD-treated neurons and in brain tissues of MCAO rats were detected. Mfn2 and miR-326-5p were reduced, and STAT3 was elevated in OGD-treated neurons and brain tissues of MCAO rats. miR-326-5p targeted and negatively regulated STAT3 expression. Restoring miR-326-5p or reducing STAT3 reinforced viability, inhibited apoptosis and oxidative stress, increased mitochondrial membrane potential and increased Mfn2 expression in OGD-treated neurons. Up-regulating miR-326-5p or down-regulating STAT3 relieved pathological changes, inhibited apoptosis and elevated mitochondrial membrane potential and Mfn2 expression in brain tissues of rats with MCAO. This study elucidates that up-regulated miR-326-5p or down-regulated STAT3 protects against CI/RI by elevating Mfn2 expression.

Keywords: Cerebral ischemia reperfusion injury, MicroRNA-326-5p, Signal transducer and activator of transcription-3, Mitofusin-2, Apoptosis, Viability

Introduction

Cerebral ischemia/reperfusion injury (CI/RI) is a kind of brain injury followed by ischemic stroke [1]. The most characteristic feature of cerebral I/R is initial transient cerebral ischemia following reperfusion [2]. CI/RI activates neuronal apoptosis and leads to hippocampal and cortical damage [3]. At present, the most common clinical application is thrombolytic for CI/RI [4]. However, reperfusion would increase the production of reactive oxygen species (ROS), leading to intracellular DNA damage, oxidative stress-related damage, protein oxidation and lipid peroxidation, thus further deteriorating blood–brain barrier and edema [5]. Thus, the urgency to search for new targeted options tops the priority for CI/RI.

MicroRNAs (miRNAs) are extensively considered as potential and prognostic roles in CI/RI [6, 7]. For example, an article has demonstrated that miR-202-5p attenuates neuronal damage and neurological deficits, as well

*Correspondence: Tangtieyu233@outlook.com
[2] Department of Neurology, Affiliated Hospital of Yangzhou University; Yangzhou University, 45 Taizhou Road, Yangzhou 225001, Jiangsu, People's Republic of China
Full list of author information is available at the end of the article

as oxygen and glucose deprivation (OGD)-induced cell damage in middle cerebral artery occlusion (MCAO) model rats in ischemic injury [8]. Additionally, it is found that up-regulation of miR-98 improves neurological outcomes in mice with I/R stroke [9] and overexpression of miR-451 alleviates ischemic cerebral apoptosis in mice with CI/RI [10]. Specifically, miR-326-5p has pro-angiogenic ability for endothelial progenitor cells and could improve cardiac function after acute myocardial infarction [11]. However, the study pivoting on miR-326-5p in CI/RI is still in its infancy. Signal transducers and transcriptional activator (STAT) are an unique family of proteins that is activated by CI/RI [12]. STAT3 was predicted as a target of miR-326-5p on the bioinformatics website; thus, we studied the role of miR-326-5p-mediated STAT3 in CI/RI. STAT3 deteriorates ischemic neuro-inflammatory processes and secondary brain injury by releasing pro-inflammatory mediators [13, 14]. Specifically, Janus-activated kinase 2(JAK2)/STAT3 pathway plays a functional role in blocking cell apoptosis induced by CI/RI [15]. Mitofusin-2 (Mfn2) is a mitochondrial fusion factor that could protect against cardio-cerebrovascular I/RI [16] and ameliorate hypoxia-induced neuronal apoptosis in ischemic brain damage [17]. It has been also recorded that Mfn2 exerts protective effect on CI/RI [18].

In a word, less in-depth investigation has discovered the combined role of miR-326-5p and STAT3 in CI/RI. Given that, this study is launched with the hypothesis that miR-326-5p attenuates CI/RI via targeting STAT3.

Materials and Methods

Ethics Statement

The experiments were approved by the Animal Care and Use Committee of Affiliated Hospital of Yangzhou University; Yangzhou University, and it was carried out with the Guide to the Care and Use of Experimental Rats of Affiliated Hospital of Yangzhou University; Yangzhou University.

Experimental Animals

Male adult Sprague–Dawley rats (6–8 weeks old, 250 ± 30 g) from the Centre of Comparative Medicine, Yangzhou University (Yangzhou, China), were kept in a specific pathogen-free environment with free access to food and water, (24 ± 1)°C, (50 ± 5)% humidity and 12-h light/dark cycle.

Cell Isolation and Identification

The rats were euthanized by decapitation, and their brains were cut into 1 mm^3 to configure cell suspensions, which were mixed with 0.4% trypan blue solution at 9:1 (the final concentration of trypan blue was 0.04%) and the cell density and survival rate were calculated by a hemocytometer. The cells (1×10^6 cells/mL) were seeded in a cell culture flask pre-coated with L-polylysine (0.1 mg/mL) at 5×10^6 cells per flask. When the cells adhered to walls, they were incubated with the renewed medium (NeurobasalA + B27 + L-glutamine) and continuously cultured for 6–7 d with the medium changed in half every 2–3 d.

Cell identification: Rat cortical neurons were utilized to prepare neuron slides which were incubated with the primary rabbit anti-rat Nestin (NES) polyclonal antibody (1:200), as well as the fluorescein isothiocyanate (FITC)-labeled goat anti-rabbit immunoglobulin *G* (1:50, both from Cell Signaling Technology, Beverly, MA, USA). Afterward, the cells were sealed with an anti-fluorescent quencher and observed by a fluorescence microscopy.

OGD Model Establishment

Neurons were cultured in a glucose-free Earle's solution and exposed to a mixed gas of 95% N_2 and 5% CO_2. After 30 min of positive pressure ventilation, a hypoxic environment was formed in which the cells were incubated (ischemia simulation by OGD in vitro). After 90 min of incubation, the cells were incubated with the maintenance cell medium after the glucose-free Earle's solution was removed. The cells were routinely cultured for subsequent experiments (reperfusion simulation by oxygen-glucose reperfusion in vitro). The normal medium under normoxia served as the control.

Neurons were divided into the control group; the OGD group, the negative control (NC) group (OGD-treated neurons transfected with scrambled oligonucleotides), the miR-326-5p agomir group (OGD-treated neurons transfected with miR-326-5p agomir), the sh-STAT3 group (OGD-treated neurons transfected with STAT3 shRNA) and the miR-326-5p agomir + overexpression (oe)-STAT3 group (OGD-treated neurons transfected with miR-326-5p agomir and pcDNA-STAT3 vector). Oligonucleotides and vectors were all provided by GenePharma (Shanghai, China).

Using lipofectamine 2000 (Invitrogen; Thermo Fisher Scientific), scrambled oligonucleotides, miR-326-5p agomir, STAT3 shRNA or miR-326-5p agomir and pcDNA-STAT3 were transfected into primary rat neurons and the transfection efficacy was tested by reverse transcription quantitative polymerase chain reaction (RT-qPCR) or Western blot after 48 h.

3-(4, 5-Dimethylthiazol-2-yl)-2, 5-Diphenyltetrazolium Bromide (MTT) Assay

Neurons were made to a suspension at 1×10^6 cells/mL and cultured for 0, 24 and 48 h, respectively. In a sterile environment, neurons were incubated for 2–4 h in 10% MTT solution and added with 150 μL Formanzan

dissolved solution (Dimethyl Sulfoxide) until the crystal was sufficiently dissolved. The optical density (OD) value was measured on a microplate reader at 570 nm.

Flow Cytometry Apoptosis Assay

Neurons were detached with 0.25% trypsin, centrifuged at 2000 rpm and resuspended in PBS. Then, neurons were centrifuged at 2000 rpm, and the pellet was resuspended by binding buffer and incubated successively with 5 μL Annexin V-FITC and 5 μL propidium iodide (PI). A flow cytometer was applied to detect apoptosis rate.

JC-1 Mitochondrial Membrane Potential Detection

Cells in the 6-well plate were rinsed with PBS, added with 1 mL cell culture medium and 1 mL JC-1 staining working solution (50 μL JC-1, 8 mL ultrapure water and 2 mL JC-1 staining buffer) (SolarbioScience, Beijing, China) and incubated for 15 min. The 1 × JC-1 staining buffer was configured by 4 mL distilled water and 1 mL JC-1 staining buffer. After incubation, cells were trypsinized, resuspended in JC-1 buffer, and tested on a flow cytometer. The relative proportion of green fluorescence was calculated.

Oxidative Stress Detection

Intracellular ROS levels were measured by 2,7-dichlorofluorescein diacetate (DCF-DA) Detection Kit (Abcam). In short, neurons were detached with 0.25% trypsin, resuspended and incubated with 10 μm DCF-DA for 30 min. After that, DCF fluorescence with excitation/emission light at 495 nm/529 nm was measured by fluorescence spectroscopy (BD Biosciences).

Detection of intracellular malondialchehyche (MDA), glutathione (GSH) contents and superoxide dismutase (SOD) activity was detected by chemical colorimetry using commercial assay kits (Beyotime Biotechnology Co., Shanghai, China). OD value was measured by a microplate reader.

Rat Model Establishment

Rats were anesthetized by intraperitoneal injection of pentobarbital sodium (50 μg/kg). A midline incision was made on the neck, the external carotid was ligated, and the common carotid artery was blocked with an arterial clip. A 3–0 silicone-coated monofilament nylon suture was carefully inserted into the internal carotid artery until light resistance. After 90 min of transient cerebral ischemia, the suture was withdrawn, and reperfusion was performed for another 24 h. The sham group received the same treatment, except that the suture did not enter the internal carotid artery. During the operation, a thermostatic bed was used to maintain the rectal temperature at 37 ± 0.5 °C [19].

Rats were allocated into 6 groups (n = 6) and injected with plasmid or miR into lateral cerebroventricular before the establishment of MCAO models, including the sham group, the MCAO group (modeled rats), the NC group (modeled rats with lateral cerebroventricular injection of 5 μL scrambled oligonucleotides [100 μM]), the miR-326-5p agomir group (modeled rats with lateral cerebroventricular injection of 5 μL miR-326-5p agomir [100 μM]), the sh-STAT3 group (modeled rats with lateral cerebroventricular injection of 5 μL STAT3 interference vector [100 μM]) and the miR-326-5p agomir + oe-STAT3 group (modeled rats with lateral cerebroventricular injection of 5 μL miR-326-5p agomir [100 μM] and 5 μL STAT3 overexpression vector [100 μM]) [20, 21].

Specimen Collection

Rats were euthanized by anesthesia, the hearts were perfused, and the entire brains were obtained. The brain injured tissues were cut into $1 \times 1 \times 1$ mm^3 tissue masses for paraffin section preparation, RT-qPCR, western blot analysis and mitochondrial membrane potential detection.

Detection of Mitochondrial Membrane Potential in Cerebral Cortex

Cerebral cortex of SD rats was separated and cut into 1 mm^3. The tissue blocks were placed on a 300 mesh nylon net and added with PBS. Then, the cell suspension was centrifuged at 1000 r/min, added with 70% ethanol and centrifuged at 1000 r/min again. Afterward, the sample was resuspended in 1 mL of PBS, and the suspension (1×10^6 cells, 100 μL) was reacted with Rhodamine123 dye solution (10 μL, 5 μg/mL) and analyzed on a flow cytometer at 488 nm.

HE Staining

The rat brain tissue was immersed in 4% paraformaldehyde for 24 h, and paraffin sections were prepared, cut into 4 μm, spread in 40 °C water and baked at 60 °C. Routinely dewaxed and hydrated, the paraffin sections were stained by HE staining solution. After HE staining, the damaged neurons showed contraction of the nucleus, cellular edema, vacuolization and darkened nuclei. The light microscope (Nikon, Japan) was used to obtain the image, and the number of surviving neurons (mm^2) of the ischemic cortex was counted.

TUNEL Staining

The paraffin sections were dewaxed and dehydrated with 100%, 95%, 80% and 70% alcohol. Then, the sections were immersed in 4% paraformaldehyde which was followed by incubation with 0.1% Triton X-100 sodium

citrate buffer for 20 min and TUNEL reaction mixture for 1–1.5 h. Next, the sections were developed by peroxidase solution and diaminobenzidine (DAB), counterstained by hematoxylin, dehydrated by gradient alcohol, permeabilized, and sealed in neutral gum. The sections were observed under a light microscope to count TUNEL-positive cells. Brownish yellow particles in the nucleus were defined as TUNEL-positive cells (apoptotic cells).

Immunohistochemistry

The sections were dewaxed, hydrated and retrieved by citrate antigen, and the endogenous catalase was blocked by 3% H_2O_2. Each sections was added with goat serum (50 μL), incubated with the primary antibody (50 μL) and reacted with the secondary antibody (50 μL) and horseradish-peroxidase-labeled streptavidin (50 μL). The sections were developed by DAB and counterstained by hematoxylin, which was followed by gradient alcohol dehydration, xylene permeabilization and neutral gum sealing. The sections were observed by a microscope (cytoplasm or nucleus of ischemic brain tissues was yellow or brownish-yellow particles). OD values were measured and averaged.

RT-qPCR

Total RNA extraction from tissues and cells was performed by Trizol (Invitrogen). mRNA expression was analyzed through qPCR using SYBR Green PCR Mix (Applied Biosystems, CA, USA) and QuantStudio TM 6Flex real-time PCR system (Applied Biosystems). Specific stem-loop reverse transcription primers and forward/reverse primers (BioTNT, Shanghai, China) were designed to analyze miRNA levels. Table 1 listed all primers. The $2^{-\triangle\triangle CT}$ method was adopted to calculate miRNA or mRNA levels.

Western Blot Analysis

The protein samples were separated by 10% sodium dodecyl sulphate polyacrylamide gel electrophoresis and electroblotted onto a polyvinylidene fluoride (PVDF) membrane. After that, the PVDF membrane was blocked with 5% skim milk powder in Tris-containing saline, probed with the primary antibodies and re-probed with the secondary antibody for 2 h. Then, the protein bands were analyzed with alkaline phosphatase buffer containing Nitroblue tetrazolium chloride and 5-Bromo-4-Chloro-3-Indolyl Phosphate and quantified by ImageJ software (NIH, Bethesda, MD, USA). The main antibodies were STAT3 (1:1000), Mfn2 (1:1000, Abcam, MA, USA) and glyceraldehyde-3-phosphate dehydrogenase (GAPDH) (1:1000, Cell Signaling Technology, Beverly, MA, USA).

Table 1 Primer sequence

Gene	Primers
miR-326-5p	Reverse transcription
	CTCAACTGGTGTCGTGGAGTCGGCAATTCAGTTGAGTTC ACAAA
	Forward: 5′-CAGGGCCTTTGTGAA-3′
	Reverse: 5′-TCAACTGGTGTCGTGG-3′
	Reverse transcription:
	CTCAACTGGTGTCGTGGAGTCGGCAATTCAGTTGAGAAA ATATG
RNU6B	Forward: 5′-CAAATTCGTGAAGCGTT-3′
	Reverse: 5′-TGGTGTCGTGGAGTCG-3′
Bax	Forward: 5′-AAGAAGCTGAGCGAGTGTCT-3′
	Reverse: 5′- CAAAGATGGTCACTGTCTGC-3′
Bcl-2	Forward: 5′- GAGCGTCAACAGGGAGATGT-3′
	Reverse: 5′- CAGCCAGGAGAAATCAAACAG-3′
STAT3	Forward: 5′-AAACTGCTTGCCTTGACCAC-3′
	Reverse: 5′-CGCCTTGCCTTCCTAAATAC-3′
GAPDH	Forward: 5′-TTCCTACCCCCAATGTATCCG-3′
	Reverse: 5′-CCACCCTGTTGCTGTAGCCATA-3′

miR-326-5p, microRNA-326-5p; STAT3, Signal transducer and activator of transcription-3; GAPDH, glyceraldehyde-3-phosphate dehydrogenase

Dual Luciferase Reporter Gene Assay

The STAT3 3′UTR containing miR-326-5p wild-type (WT) or mutant (Mut) binding sites was cloned into pmirGLO vector (Promega, WI, USA), named as STAT3-WT and STAT3-Mut. Cells were seeded in a 24-well plate at 2×10^4 cells/well and co-transfected with 100 ng of STAT3-WT or STAT3-Mut luciferase vector and 50 nM miR-326-5p agomir or it agomir NC at 70% confluence. Luciferase activity was measured using the Dual-Luciferase Reporter Assay System (Promega Corporation, WI, USA).

Statistical Analysis

SPSS 21.0 (IBM, NY, USA) statistical software was used for data analysis. The data were expressed as mean ± standard deviation (SD). The difference between two groups was analyzed by Student's t-test, while multiple comparisons were analyzed by one-way analysis of variance (ANOVA), followed by Tukey's post hoc test. P represented two-sided test, and $P < 0.05$ was considered of statistically significance.

Results

Up-regulation of miR-326-5p or Down-Regulation of STAT3 Attenuates Apoptosis of OGD-Treated Cortical Neurons

Cultured for a week, the rat cortical neurons were differentiated and matured. Microscopically, the neurons

showed larger neuron bodies, more transparent cytoplasm, large nucleus with low density, and strong refractive index. The neuron bodies were conical or round, and the dendrites were staggered and adhered to walls (Fig. 1a, b). NES was a specific chemical marker of cerebral neurons to locate neurons with high specificity through immunofluorescence assay. Neurons were found to specifically bind to NES and showed green fluorescence (Fig. 1c).

MTT assay was applied to detect cortical neuron viability (Fig. 1d). The results demonstrated that rat cortical neuron viability was impaired in the OGD group and the miR-326-5p agomir + oe-STAT3 group versus the control group and the miR-326-5p agomir group, but enhanced in the miR-326-5p agomir group and sh-STAT3 group versus the NC group (all $P < 0.05$).

Rat cortical neuron apoptosis was determined by flow cytometry, while Bcl-2 and Bax mRNA expression by RT-qPCR (Fig. 1e–g). The results explained that in comparison with the control group and the miR-326-5p agomir group, the OGD group and the miR-326-5p agomir + oe-STAT3 group demonstrated increased apoptosis rate, reduced Bcl-2 expression and increased Bax expression (all $P < 0.05$). With the NC groups by contrast, the apoptosis rate was lowered, Bcl-2 level was elevated and Bax level was suppressed in the miR-326-5p agomir group and the sh-STAT3 group (all $P < 0.05$).

Up-regulation of miR-326-5p or Down-Regulation of STAT3 Increases Mfn2 and Mitochondrial Membrane Potential Level in Cortical Neurons After OGD Injury

Mfn2 expression in OGD-treated cortical neurons was detected by western blot analysis (Fig. 2a, b). With respect to the control group and the miR-326-5p agomir group, Mfn2 protein expression reduced in the OGD group and miR-326-5p agomir + oe-STAT3 group, while increased in the miR-326-5p agomir group and sh-STAT3 group versus the NC group (all $P < 0.05$).

Mitochondrial membrane potential detected by JC-1 found that (Fig. 2c, d) with respect to the control group and miR-326-5p agomir group, the mitochondrial membrane potential level decreased in the OGD group and the miR-326-5p agomir + oe-STAT3 group (all $P < 0.05$). Relative to the NC groups, mitochondrial membrane

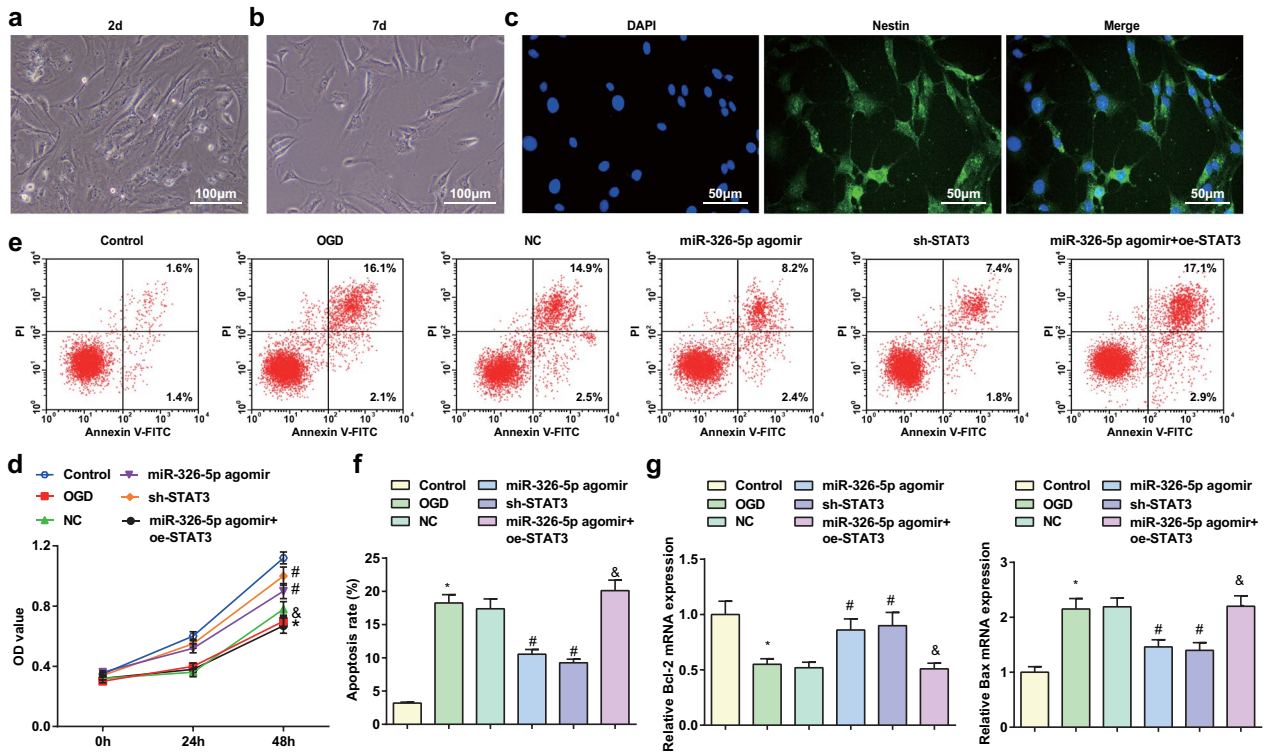

Fig. 1 Up-regulation of miR-326-5p or down-regulation of STAT3 attenuates apoptosis of OGD-treated cortical neurons. **a** Cerebral neurons with 2-d adherent culture (scale bar: 100 μm); **b** Cerebral neurons with 7-d adherent culture (scale bar: 100 μm); **c** Cerebral neurons with 7-d adherent culture stained by NES immunofluorescence assay (scale bar: 50 μm); **d** Viability of OGD-treated cortical neurons by MTT assay; **e** Apoptosis of OGD-treated cortical neurons detected by flow cytometry; **f** Apoptosis rate of OGD-treated cortical neurons; **g** Bcl-2 and Bax mRNA expression in OGD-treated cortical neurons; *$P < 0.05$ compared with the control group; #$P < 0.05$ compared with the NC group; &$P < 0.05$ compared with the miR-326-5p agomir group

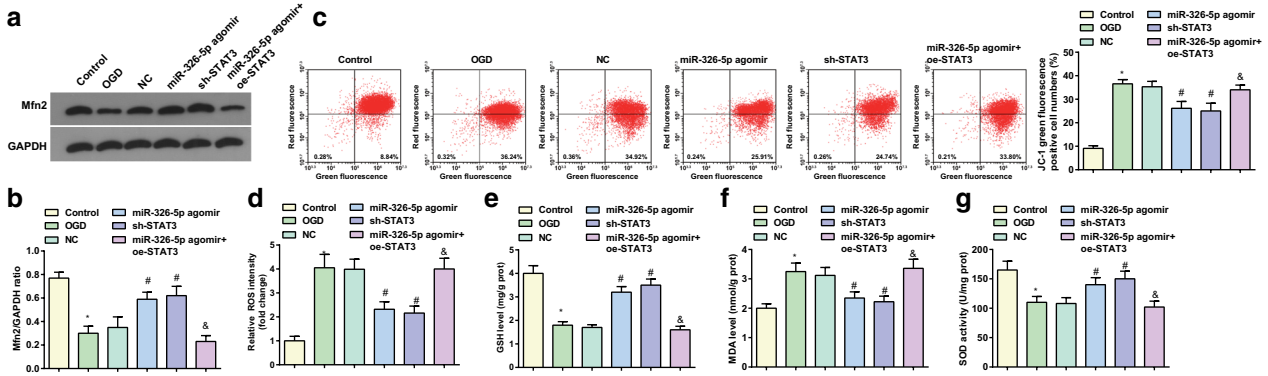

Fig. 2 Up-regulation of miR-326-5p or down-regulation of STAT3 increases Mfn2 and mitochondrial membrane potential level in OGD-treated cortical neurons. **a**, **b** Mfn2 protein expression in OGD-treated cortical neurons; **c** JC-1 flow cytometry of mitochondrial membrane potential level in OGD-treated cortical neurons; **d** ROS content in OGD-treated cortical neurons after up-regulating miR-326-5p or down-regulating STAT3; **e** GSH activity in OGD-treated cortical neurons after up-regulating miR-326-5p or down-regulating STAT3; **f** MDA content in OGD-treated cortical neurons after up-regulating miR-326-5p or down-regulating STAT3; **g** SOD activity in neurons after up-regulating miR-326-5p or down-regulating STAT3; *$P < 0.05$ compared with the control group; #$P < 0.05$ compared with the NC group; &$P < 0.05$ compared with the miR-326-5p agomir group

potential level increased in the miR-326-5p agomir group and sh-STAT3 group (all $P < 0.05$).

ROS and MDA contents, and GSH and SOD activities in OGD-treated cortical neurons were determined and the results indicated that versus the control group and the miR-326-5p agomir group, the OGD group and the miR-326-5p agomir + oe-STAT3 group presented increased ROS and MDA contents and impaired GSH and SOD activities (all $P < 0.05$). In comparison with the NC groups, the miR-326-5p agomir group and sh-STAT3 group showed reduced ROS and MDA contents and reinforced GSH and SOD activities (all $P < 0.05$) (Fig. 2e–g).

Up-regulation of miR-326-5p or Down-Regulation of STAT3 Impedes Pathological Damage of Cortical Neurons and Inhibits Apoptosis in Rats with CI/RI

HE staining was adopted to observe the pathological damage of brain tissues (Fig. 3a, b), showing that in the sham group, the neurons were normal in structure and neatly arranged with pale red cytoplasm, blue nucleus and clear nucleolus. In the MCAO group, the NC group and the miR-326-5p agomir + oe-STAT3 group, except for necrosis, it was observed that neurons were disorderly arranged and stained darker, with nuclear membrane rupture, cell structure disappearance, karyopyknosis, deep stained nucleus and lysis in a large amount. In the miR-326-5p agomir group and the sh-STAT3 group, neurons swelling was alleviated and neurons were arranged orderly, and the necrotic cells were reduced, indicating a better status in relation to the MCAO group and the NC group.

TUNEL staining was utilized for detection of neuronal apoptosis and RT-qPCR for Bcl-2 and Bax mRNA expression in brain tissues. The results displayed that (Fig. 3c–e) in comparison with the sham group and the miR-326-5p agomir group, the TUNEL-positive rate increased, Bcl-2 mRNA expression decreased and Bax mRNA expression increased in the MCAO group and the miR-326-5p agomir + oe-STAT3 group (all $P < 0.05$). Lower TUNEL-positive rate and Bax mRNA expression, and higher Bcl-2 mRNA expression showed in the miR-326-5p agomir and the sh-STAT3 group than the NC group (all $P < 0.05$).

Up-regulation of miR-326-5p or Down-Regulation of STAT3 Increases Mitochondrial Membrane Potential Level in Brain Tissues in Rats with CI/RI

Mfn2 protein expression detection in rat brain tissue was performed by immunohistochemistry, and the results displayed that (Fig. 4a, b) lower Mfn2 protein expression was tested in the sham group and the miR-326-5p agomir group versus the MCAO group and the miR-326-5p agomir + oe-STAT3 group, while higher Mfn2 protein expression was measured in the miR-326-5p agomir group and the sh-STAT3 group instead of the NC group (all $P < 0.05$).

Detection of mitochondrial membrane potential level discovered that (Fig. 4c) by comparison with the sham group and the miR-326-5p agomir group, mitochondrial membrane potential level decreased in the MCAO group and the miR-326-5p agomir + oe-STAT3 group, while it increased in the miR-326-5p agomir group and the sh-STAT3 group in contrast to the NC group (all $P < 0.05$).

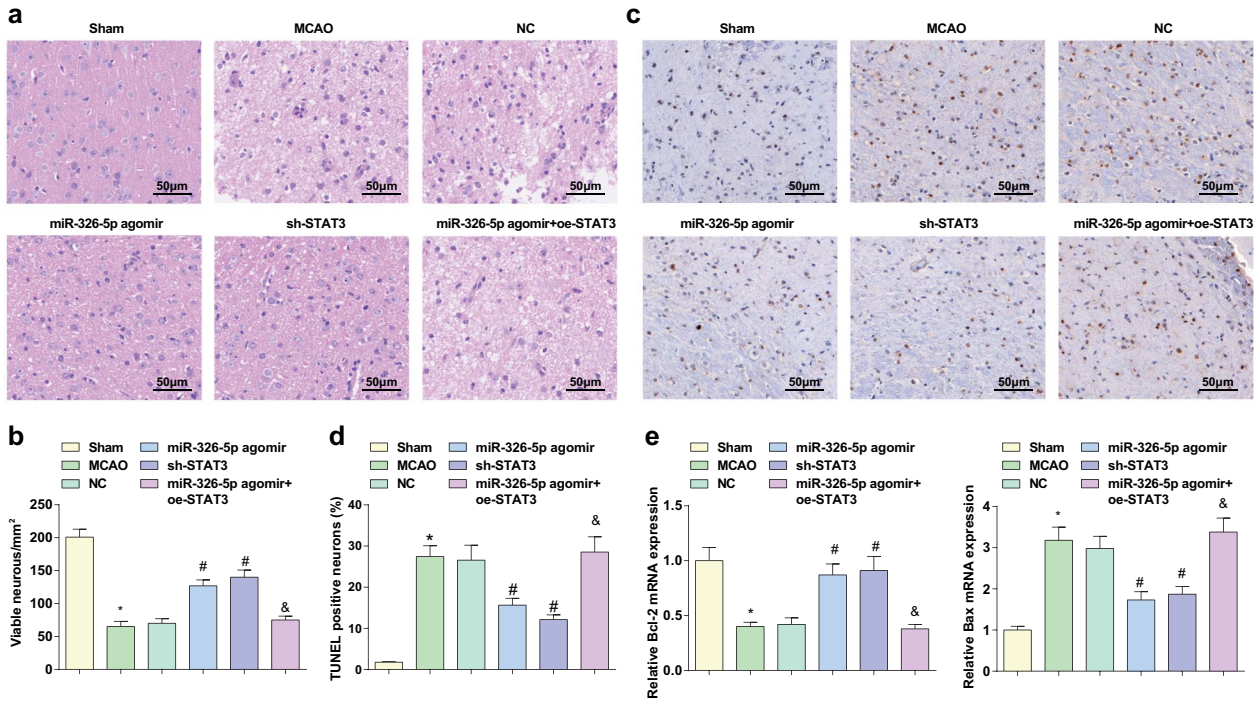

Fig. 3 Up-regulation of miR-326-5p or down-regulation of STAT3 impedes pathological damage of cortical neurons and inhibits apoptosis in rats with CI/RI. **a** Pathological damage of brain tissues in MCAO rats observed by HE staining (scale bar: 50 μm); **b** The number of intact neurons of MCAO rat brain tissues after up-regulating miR-326-5p or down-regulating STAT3; **c** Neuronal apoptosis in MCAO rat brain tissues detected by TUNEL staining (scale bar: 50 μm); **d** TUNEL-positive rates in MCAO rat brain tissues after up-regulating miR-326-5p or down-regulating STAT3; **e** Bcl-2 and Bax mRNA expression in MCAO rat brain tissues after up-regulating miR-326-5p or down-regulating STAT3; *$P < 0.05$ compared with the sham group; #$P < 0.05$ compared with the NC group; &$P < 0.05$ compared with the miR-326-5p agomir group

miR-326-5p Targets STAT3

miR-326-5p and STAT3 expression in cortical neurons and brain tissues were detected by RT-qPCR and western blot analysis. In cortical neurons in vitro, a decrease suggested in the miR-326-5p expression and an increase in the STAT3 expression in the OGD group relative to the control group (both $P < 0.05$). With respect to the NC group, miR-326-5p expression elevated and STAT3 expression reduced in the miR-326-5p agomir group (both $P < 0.05$); STAT3 expression decreased ($P < 0.05$) in the sh-STAT3 group. By contrast to the miR-326-5p agomir group, STAT3 expression was raised in the miR-326-5p agomir + oe-STAT3 group ($P < 0.05$) (Fig. 5a–c).

In brain tissues in vivo, in relation to the sham group, lower miR-326-5p and higher STAT3 appeared in the MCAO group (both $P < 0.05$). Relative to the NC group, miR-326-5p expression rose while STAT3 expression decreased in the miR-326-5p agomir group (both $P < 0.05$). STAT3 expression decreased in the sh-STAT3 group ($P < 0.05$). With the miR-326-5p agomir group by contrast, STAT3 expression elevated in the miR-326-5p agomir + oe-STAT3 group ($P < 0.05$) (Fig. 5d–f).

The potential miR-326-5p targeting sites on STAT3 3′UTR were found by DIANA and miRDB software (Fig. 5g). STAT3 3′UTR containing the WT miR-326-5p binding site and Mut binding site were constructed and inserted into the pmirGLO plasmid. The binding of miR-326-5p to STAT3 3′UTR was further validated by luciferase reporter assay. Luciferase reporter assay revealed that miR-326-5p agomir reduced the relative luciferase activity of STAT3-WT, but not STAT3-Mut (Fig. 5h), implying that STAT3 was a direct target gene of miR-326-5p.

Discussion

CI/RI is the leading cause of cerebrovascular death [22]. miRNAs are indicated to be involved in CI/RI [23]. However, the comprehensive understanding of miR-326-5p-related mechanism is still insufficient in CI/RI. Thus, this study is targeted to unearth the concrete roles of miR-326-5p in CI/RI with the emphasis on the combined reciprocal of miR-326-5p and STAT3. Productively, this study has declared that up-regulation of miR-326-5p

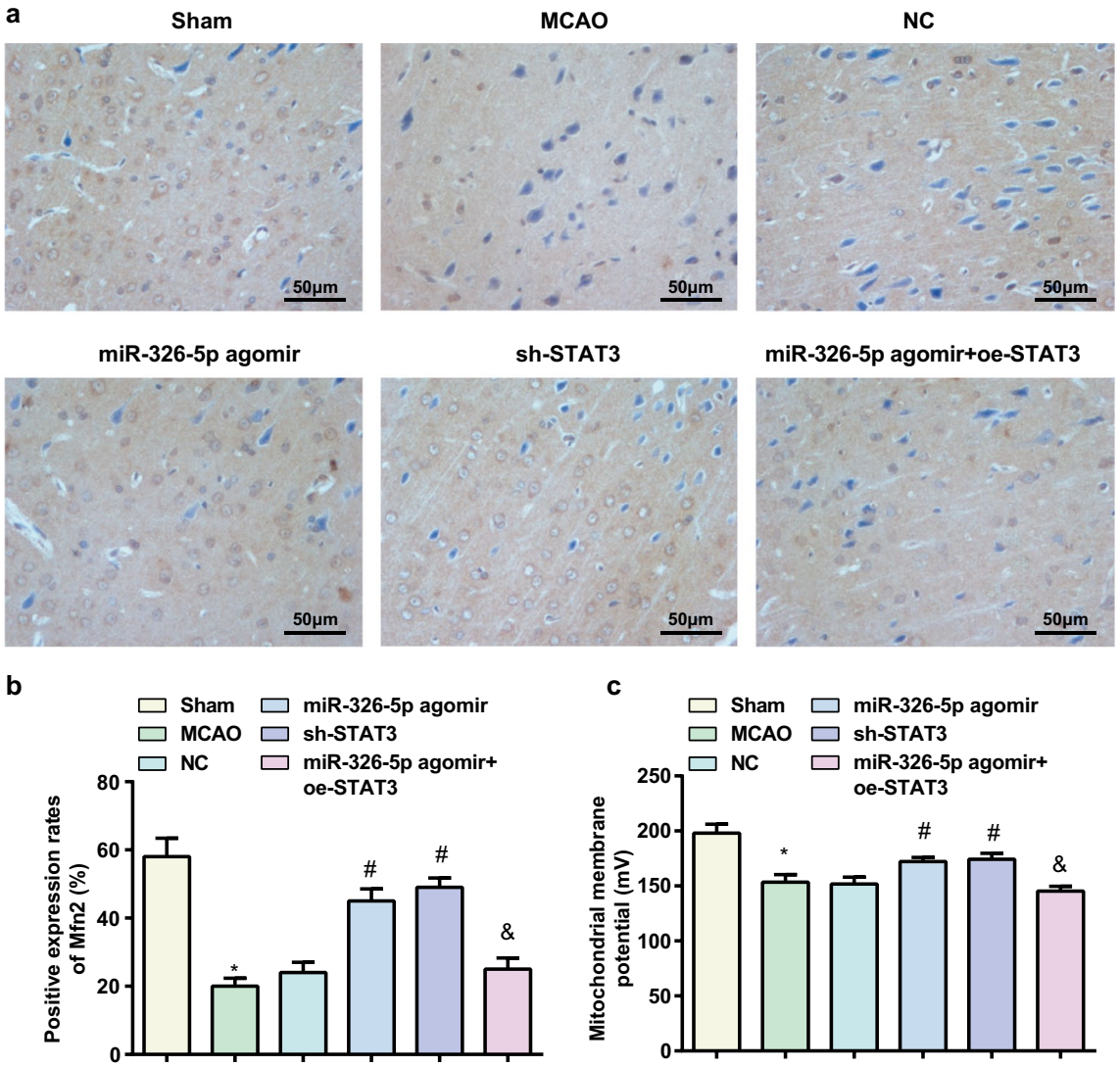

Fig. 4 Up-regulation of miR-326-5p or down-regulation of STAT3 increases mitochondrial membrane potential level in brain tissues in rats with CI/RI. **a** Mfn2 expression detected by immunohistochemistry in rat brain tissue (scale bar: 50 μm); **b** Number of Mfn2-positive cells in MCAO rat brain tissues after up-regulating miR-326-5p or down-regulating STAT3; **c** Mitochondrial transmembrane potentials in neurons of MCAO rat brain tissues after up-regulating miR-326-5p or down-regulating STAT3; *$P < 0.05$ compared with the sham group; #$P < 0.05$ compared with the NC group; &$P < 0.05$ compared with the miR-326-5p agomir group

attenuated CI/RI and elevated Mfn2 expression via STAT3 inhibition.

At the beginning, miR-326-5p expression was determined to reduce in CI/RI in vivo and in vitro. Subsequently, we arranged a series assays and found that up-regulating miR-326-5p enhanced neuron viability and mitochondrial function, elevated Mfn2 expression and restrained oxidative stress and apoptosis. Furthermore, in vivo experiments in rats further verified the functional roles of restored miR-326-5p in CI/RI. As a matter of fact, high miR-326 is proved to correlate with long overall survival of patients with glioblastoma, the common type of brain tumor [24]. Also, miR-326 expression has been further evidenced to reduce in Parkinson's disease and miR-326 could suppress apoptosis of dopaminergic neurons and reduce inflammatory response [25]. Except for that, the reduction in miR-326-5p is manifested in endothelial progenitor cells in the course of myocardial infarction, and introduction of endothelial progenitor cells overexpressing could promote cardiac function recovery [11]. There has been a study illustrating that up-regulation of miR-326 improves the behavioral function,

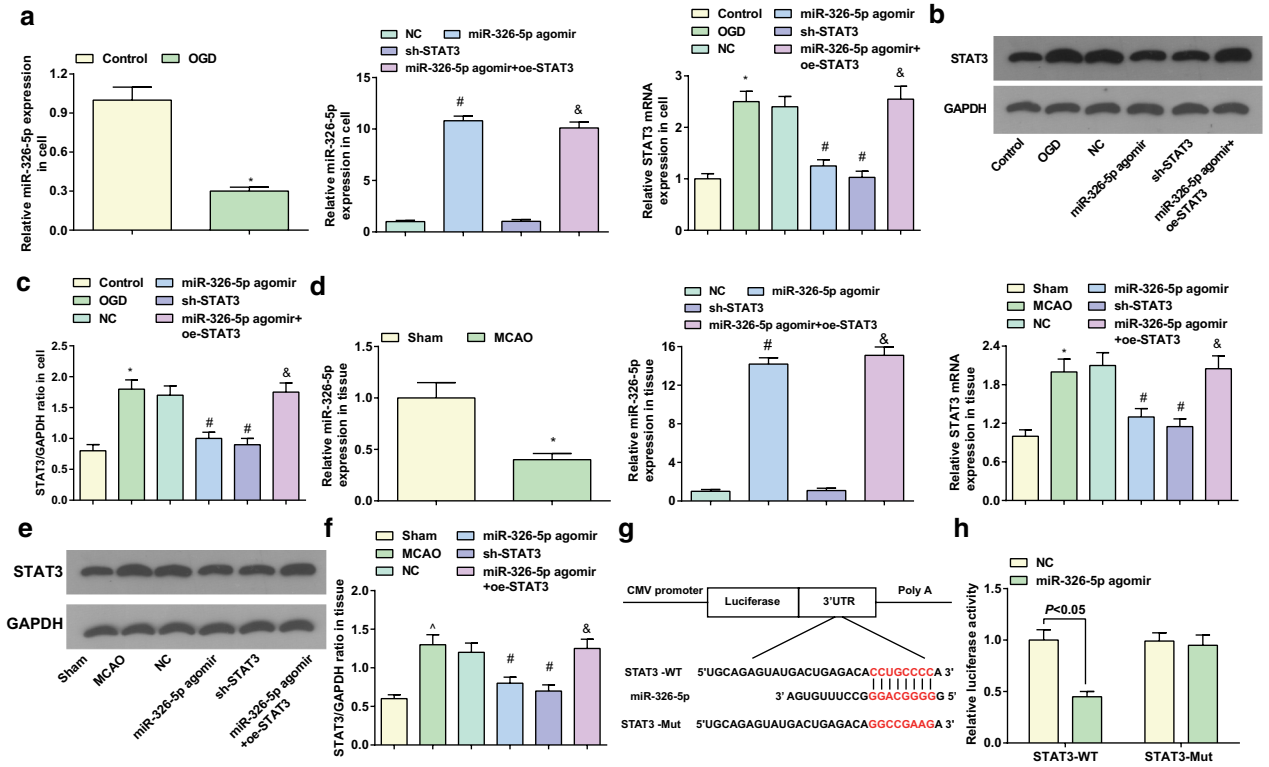

Fig. 5 miR-326-5p targets STAT3. **a** miR-326-5p and STAT3 mRNA expression in OGD-treated cortical neurons in vitro; **b**, **c** STAT3 protein expression in OGD-treated cortical neurons in vitro; **d** miR-326-5p and STAT3 mRNA expression in MCAO rat brain tissues; **e**, **f** STAT3 protein expression in MCAO rat brain tissues; **g** Predicted binding site of miR-326-5p and STAT3 by bioinformatics software; **h** The targeting relationship between miR-326-5p and STAT3 validated by dual luciferase reporter gene assay; In Figure **a**–**c**, *$P < 0.05$ compared with the control group; #$P < 0.05$ compared with the NC group; &$P < 0.05$ compared with the miR-326-5p agomir group. In Figure **d**–**f**, *$P < 0.05$ compared with the sham group; #$P < 0.05$ compared with the NC group; &$P < 0.05$ compared with the miR-326-5p agomir group

enhances neuronal viability and depresses neuronal apoptosis in mice with Alzheimer's disease [26]. Furthermore, it is documented that up-regulation of miR-326 by miR-326 mimic could suppress inducible nitric oxide synthase in dopaminergic neurons in Parkinson's disease [27].

In this study, we found that STAT3 was a target gene of miR-326-5p. Supported by an advanced study, it is indicated that STAT3 expression is negatively regulated by miR-326 in human endometrial carcinoma stem cells [28]. In the present study, we measured that STAT3 expression was enhanced in CI/RI. Currently, it has been found that I/R injury and OGD would induce STAT3 expression to increase [29]. Intriguingly, STAT3 mRNA expression trends to an increment in I/R animals [30]. Additionally, STAT3 protein expression is reported to up-regulate in CI/RI [31]. Next, our study revealed that down-regulating STAT3 had the therapeutic effects on CI/RI rats and OGD-treated neurons. As supported by a study, it is concluded that miR-31 induction discourages oxidative stress by inactivation of JAK/STAT3 pathway in ischemic stroke [32]. Also, inhibition of JAK2/STAT3 pathway is beneficial to oxidative stress impairment in CI/RI [31]. Furthermore, knockdown of JAK/STAT3 pathway is identified to enhance cell viability, and reduce oxidative stress and neuron apoptosis in ischemic brain injury [33]. Lately, inhibited JAK/STAT3 signaling pathway is witnessed to relieve myocardial infarction in myocardial I/R injury [34]. As demonstrated, depleted STAT3 undermines neuronal apoptosis in rats with white matter injury [35]. Moreover, the suppression of neuronal apoptosis, and alleviation of cerebral infarct size are attributed to JAK2/STAT3 inhibition in rats with CI/RI [36].

Finally, we focused on the effects of miR-326-5p and STAT3 on Mfn2 expression and discovered that the reduced level Mfn2 in rats with CI/RI and OGD-treated neurons could be elevated by either restoring miR-326-5p or silencing STAT3. As implicated by a previous study, it is documented that Mfn2 is decreased in the lately phase of reperfusion and poorly expressed of Mfn2 exacerbates CI/RI via restrained autophagosome formation and autophagosome and lysosome fusion [18]. Additionally,

Mfn2 is implied to reduce even disappear in I/R injury in old hepatocytes [37]. However, few researches have discussed the regulatory mechanism of miR-326-5p and STAT3 for Mfn2.

Conclusion

In general, this study has elucidated the mechanisms that elevated miR-326-5p inhibits neuronal apoptosis, attenuates pathological damage of neurons and increases the expression of Mfn2 via STAT3 downregulation in CI/RI. The study may update the potential mechanism of miR-326-5p and STAT3 in CI/RI. However, more studies are still needed for further development of the molecular mechanism in CI/RI.

Abbreviations

miRNAs: MicroRNAs; STAT3: Signal transducer and activator of transcription-3; OGD: Oxygen and glucose deprivation; MCAO: Middle cerebral artery occlusion; ROS: Reactive oxygen species; STAT: Signal transducers and transcriptional activator; Mfn2: Mitofusin-2; FITC: Fluorescein isothiocyanate; NES: Nestin; NC: Negative control; Oe: Overexpression; RT-qPCR: Reverse transcription quantitative polymerase chain reaction; OD: Optical density; PI: Propidium iodide; MDA: Malondialchehyche; GSH: Glutathione; SOD: Superoxide dismutase; DAB: Diaminobenzidine; PVDF: Polyvinylidene fluoride; WT: Wild-type; Mut: Mutant; SD: Standard deviation; ANOVA: One-way analysis of variance.

Acknowledgements

We would like to acknowledge the reviewers for their helpful comments on this paper.

Authors' contributions

Tieyu Tang contributed to study design; Yumin Huang contributed to manuscript editing; Yingge Wang, Zuowei Duan and Jingyan Liang contributed to experimental studies; Yijun Xu and Shuai Zhang contributed to data analysis. All authors read and approved the final manuscript.

Funding

This work was supported by The National Key Research and Development Program of China (Grant No. 2016YFE012600), The National Nature Science Foundation of China (Grant No. 81570392) and The Foundation of Jiangsu Provincial Commission of Health and Family Planning (QNRC2016353).

Availability of data and materials

Not applicable.

Declarations

Ethics approval and consent to participate

The experiments were approved by the Animal Care and Use Committee of Affiliated Hospital of Yangzhou University; Yangzhou University, and it was carried out in strict consistence with the Guide to the Care and Use of Experimental Rats of Affiliated Hospital of Yangzhou University; Yangzhou University.

Consent for publication

Not applicable.

Competing interests

The authors declare that they have no conflicts of interest.

Author details

[1] Department of Respiratory and Critical Medicine, Affiliated Hospital of Yangzhou University, Yangzhou University, Yangzhou 225001, People's Republic of China. [2] Department of Neurology, Affiliated Hospital of Yangzhou University; Yangzhou University, 45 Taizhou Road, Yangzhou 225001, Jiangsu, People's Republic of China. [3] Institute of Translational Medicine, Medical College, Yangzhou University, Yangzhou 225001, People's Republic of China. [4] Jiangsu Key Laboratory of Integrated Traditional Chinese and Western Medicine for Prevention and Treatment of Senile Diseases, Yangzhou University, Yangzhou 225001, People's Republic of China. [5] Department of Jiangsu Key Laboratory of Experimental, Translational Non-coding RNA Research, Yangzhou, Jiangsu 225001, People's Republic of China. [6] Medical College, Yangzhou University; Yangzhou University, Yangzhou 225001, People's Republic of China.

Received: 28 August 2020 Accepted: 30 March 2021
Published online: 20 April 2021

References

1. He Y, Jiang K, Zhao X (2020) Taraxasterol protects hippocampal neurons from oxygen-glucose deprivation-induced injury through activation of Nrf2 signalling pathway. Artif Cells Nanomed Biotechnol 48(1):252–258
2. Cheng X et al (2020) Dynamic alterations of brain injury, functional recovery, and metabolites profile after cerebral ischemia/reperfusion in rats contributes to potential biomarkers. J Mol Neurosci
3. Zhao JX et al (2011) Effects of electroacupuncture on hippocampal and cortical apoptosis in a mouse model of cerebral ischemia-reperfusion injury. J Tradit Chin Med 31(4):349–355
4. Cai HA et al (2020) Ozone alleviates ischemia/reperfusion injury by inhibiting mitochondrion-mediated apoptosis pathway in SH-SY5Y cells. Cell Biol Int 44(4):975–984
5. Kishimoto M et al (2019) Oxidative stress-responsive apoptosis inducing protein (ORAIP) plays a critical role in cerebral ischemia/reperfusion injury. Sci Rep 9(1):13512
6. Yao X et al (2019) Upregulation of miR-496 decreases cerebral ischemia/reperfusion injury by negatively regulating BCL2L14. Neurosci Lett 696:197–205
7. Huang R et al (2019) MiR-34b protects against focal cerebral ischemia-reperfusion (I/R) injury in rat by targeting keap1. J Stroke Cerebrovasc Dis 28(1):1–9
8. Li B, et al (2019) MiR-202–5p attenuates neurological deficits and neuronal injury in MCAO model rats and OGD-induced injury in Neuro-2a cells by targeting eIF4E-mediated induction of autophagy and inhibition of Akt/GSK-3beta pathway. Mol Cell Probes, p 101497.
9. Bernstein DL, et al (2019) miR-98 reduces endothelial dysfunction by protecting blood-brain barrier (BBB) and improves neurological outcomes in mouse ischemia/reperfusion stroke model. J Cereb Blood Flow Metab, 2019: p. 271678X19882264.
10. Fu C et al (2019) Potential neuroprotective effect of miR-451 against cerebral ischemia/reperfusion injury in stroke patients and a mouse model. World Neurosurg 130:e54–e61
11. Li X et al (2019) MicroRNA-326-5p enhances therapeutic potential of endothelial progenitor cells for myocardial infarction. Stem Cell Res Ther 10(1):323
12. Wu WJ et al (2017) Diffusion-weighted magnetic resonance imaging reflects activation of signal transducer and activator of transcription 3 during focal cerebral ischemia/reperfusion. Neural Regen Res 12(7):1124–1130
13. Yu L et al (2013) Neuroprotective effect of kaempferol glycosides against brain injury and neuroinflammation by inhibiting the activation of NF-kappaB and STAT3 in transient focal stroke. PLoS ONE 8(2):e55839
14. Zheng T et al (2019) Cornel iridoid glycoside exerts a neuroprotective effect on neuroinflammation in rats with brain injury by inhibiting NF-kappaB and STAT3. 3 Biotech, 2019. **9**(5): p. 195.
15. Hu GQ et al (2017) Inhibition of cerebral ischemia/reperfusion injury-induced apoptosis: nicotiflorin and JAK2/STAT3 pathway. Neural Regen Res 12(1):96–102
16. Liu M, Li X, Huang D (2020) Mfn2 overexpression attenuates cardio-cerebrovascular ischemia-reperfusion injury through mitochondrial fusion and activation of the AMPK/Sirt3 signaling. Front Cell Dev Biol 8:598078
17. Peng C et al (2015) Mitofusin 2 ameliorates hypoxia-induced apoptosis via mitochondrial function and signaling pathways. Int J Biochem Cell Biol 69:29–40

18. Peng C et al (2018) Mitofusin 2 exerts a protective role in ischemia reperfusion injury through increasing autophagy. Cell Physiol Biochem 46(6):2311–2324
19. Xu Y et al (2017) YiQiFuMai powder injection protects against ischemic stroke via inhibiting neuronal apoptosis and PKCdelta/Drp1-mediated excessive mitochondrial fission. Oxid Med Cell Longev 2017:1832093
20. Mo JL et al (2018) MicroRNA-365 modulates astrocyte conversion into neuron in adult rat brain after stroke by targeting Pax6. Glia 66(7):1346–1362
21. Piao JM et al (2018) MicroRNA-381 favors repair of nerve injury through regulation of the SDF-1/CXCR4 signaling pathway via LRRC4 in acute cerebral ischemia after cerebral lymphatic blockage. Cell Physiol Biochem 46(3):890–906
22. Zhai Y et al (2020) Dexmedetomidine post-conditioning alleviates cerebral ischemia-reperfusion injury in rats by inhibiting high mobility group protein B1 group (HMGB1)/toll-like receptor 4 (TLR4)/nuclear factor kappa B (NF-kappaB) signaling pathway. Med Sci Monit 26:e918617
23. Zhu X et al (2019) MiR-153 regulates cardiomyocyte apoptosis by targeting Nrf2/HO-1 signaling. Chromosome Res 27(3):167–178
24. Qiu S et al (2013) Interactions of miR-323/miR-326/miR-329 and miR-130a/miR-155/miR-210 as prognostic indicators for clinical outcome of glioblastoma patients. J Transl Med 11:10
25. Zhang Y et al (2019) MicroRNA-326 inhibits apoptosis and promotes proliferation of dopaminergic neurons in parkinson's disease through suppression of KLK7-mediated MAPK signaling pathway. J Mol Neurosci 69(2):197–214
26. He B et al (2020) MicroRNA-326 decreases tau phosphorylation and neuron apoptosis through inhibition of the JNK signaling pathway by targeting VAV1 in Alzheimer's disease. J Cell Physiol 235(1):480–493
27. Zhao XH et al (2019) MicroRNA-326 suppresses iNOS expression and promotes autophagy of dopaminergic neurons through the JNK signaling by targeting XBP1 in a mouse model of Parkinson's disease. J Cell Biochem 120(9):14995–15006
28. Gao Y et al (2019) Superparamagnetic iron oxide nanoparticle-mediated expression of miR-326 inhibits human endometrial carcinoma stem cell growth. Int J Nanomedicine 14:2719–2731
29. Chen J et al (2019) EZH2 inhibitor DZNep modulates microglial activation and protects against ischaemic brain injury after experimental stroke. Eur J Pharmacol 857:172452
30. Athanasopoulos P et al (2016) Expression of inflammatory and regenerative genes in a model of liver ischemia/reperfusion and partial hepatectomy. J Invest Surg 29(2):67–73
31. Wang RX, Li S, Sui X (2019) Sodium butyrate relieves cerebral ischemia-reperfusion injury in mice by inhibiting JNK/STAT pathway. Eur Rev Med Pharmacol Sci 23(4):1762–1769
32. Li J, Lv H, Che YQ (2020) Upregulated microRNA-31 inhibits oxidative stress-induced neuronal injury through the JAK/STAT3 pathway by binding to PKD1 in mice with ischemic stroke. J Cell Physiol 235(3):2414–2428
33. Zhou B, Liu HY, Zhu BL (2019) Protective role of SOCS3 modified bone marrow mesenchymal stem cells in hypoxia-induced injury of PC12 cells. J Mol Neurosci 67(3):400–410
34. Zhang WY, Zhang QL, Xu MJ (2019) Effects of propofol on myocardial ischemia reperfusion injury through inhibiting the JAK/STAT pathway. Eur Rev Med Pharmacol Sci 23(14):6339–6345
35. Chen XM et al (2019) Effect of the JAK2/STAT3 signaling pathway on nerve cell apoptosis in rats with white matter injury. Eur Rev Med Pharmacol Sci 23(1):321–327
36. Hou Y et al (2018) Resveratrol provides neuroprotection by regulating the JAK2/STAT3/PI3K/AKT/mTOR pathway after stroke in rats. Genes Dis 5(3):245–255
37. Chun SK et al (2018) Loss of sirtuin 1 and mitofusin 2 contributes to enhanced ischemia/reperfusion injury in aged livers. Aging Cell 17(4):e12761

Publisher's Note